Dye-Assisted Structural Modulation of Hydrogen-Bonded Binary Supramolecular Polymers

Shiki Yagai,* Masatsugu Higashi, Takashi Karatsu, and Akihide Kitamura*

Department of Applied Chemistry and Biotechnology, Faculty of Engineering, Chiba University, 1-33 Yayoi-cho, Inage-ku, Chiba 263-8522, Japan

Received May 17, 2005. Revised Manuscript Received June 23, 2005

Binary hydrogen-bonded supramolecular polymers composed of a dimeric melamine (bis(melamine)) and barbiturate-type merocyanine dyes are prepared in aliphatic solvents. Macroscopic structure and rheological behavior of the supramolecular polymers are investigated by scanning electron microscopic observation and dynamic rheological measurement. Despite conformational flexibility in the bis(melamine) component, supramolecular polymers exhibit well-defined one-dimensional fibrous or two-dimensional sheetlike macroscopic structures, which are dependent on the blended merocyanine dyes. UV−vis studies of the supramolecular polymerization in dilute solutions imply that the merocyanine dyes exist as self-aggregated state upon supramolecular polymerization with the bis(melamine) component. This observation strongly suggests the presence of secondary structures of the quasi-one-dimensional flexible supramolecular polymers.

Introduction

Organizations of biopolymers into well-defined higher-order structures through inter- and/or intramacromolecular noncovalent interactions are prerequisite to generate sophisticated biological functions. α-Helices and β-sheets of natural proteins are typical examples for such organized biomolecules.[1] Conventional synthetic polymers also adopt noncovalent interactions, which determine their material properties. Creation of polymers applicable to templates for inorganic materials and anisotropic mass-transporting materials requires well-defined macroscopic structures. Such macroscopically ordered structures may not be created from randomly coiled flexible polymers but may be created from those polymers featuring well-defined secondary structures supported by specific noncovalent interactions such as intrachain association (folding) or directional interchain association.[2] Thus, construction of well-defined secondary structures requires uniform introduction of effective interactive sites into polymer main chains.[3]

The concept of supramolecular polymers enables facile preparation of those polymers capable of forming secondary structures.[4] The noncovalent polymerization of specifically designed building blocks provides quasi-one-dimensional supramolecular polymers with uniformly located additional interactive sites. For example, Meijer and co-workers have exploited quadruple hydrogen-bonded supramolecular polymers where the hydrogen-bonded planar segments intrasupramolecularly stack up to give cylindrical secondary structures.[5] Use of aggregate-forming dyes and π-conjugated systems as building blocks facilitates directed formation of secondary structures as well as gives rise to highly organized dye assemblies applicable to processible organic optoelectronic devices.[6]

Previously, we reported supramolecular polymers based on bis(melamine) **1** that can noncovalently polymerize upon binding with cyanurates or barbiturates through complementary triple hydrogen-bonding interaction (Figure 1a).[7] These supramolecular polymers has potential ability to organize into macroscopically well-defined structures because they comprise melamine·cyanurate·melamine hydrogen-bonded planar segments which can act as an additional π−π stacking interactive sites (Figure 1b).[8] However, use of nonchromophoric *N*-dodecylcyanurate resulted in irregular macroscopic morphologies as observed by scanning electron microscopy.[7] This is probably due to the absence of secondary structures in the supramolecular polymers. Thus, stronger and directional aromatic stacking interaction between hydrogen-bonded planar segments might be required

* To whom correspondence should be addressed. E-mail: yagai@faculty.chiba-u.jp (S.Y.).

(1) Dill, K. A. *Biochemistry* **1990**, *29*, 7133−7155.
(2) (a) Muthukumar, M.; Ober, C. K.; Thomas, E. L. *Science* **1997**, *277*, 1225−1232. (b) Gellman, S. H. *Acc. Chem. Res.* **1998**, *31*, 173−180. (c) Hill, D. J.; Mio, M. J.; Prince, R. B.; Hughes, T. S.; Moore, J. S. *Chem. Rev.* **2001**, *101*, 3893−4011. (d) Li, A. D. Q.; Wang, W.; Wang, L.-Q. *Chem.*—Eur. J. **2003**, *9*, 4594−4601. (e) Huc, I. *Eur. J. Org. Chem.* **2004**, 17−29. (f) Lee, M.; Cho, B.-K.; Zin, W.-C. *Chem. Rev.* **2001**, *101*, 3869−3892. (g) Klok, H.-A.; Lecommandoux, S. *Adv. Mater.* **2001**, *13*, 1217−1229. (h) Ikkala, O.; ten Brinke, G. *Chem. Commun.* **2004**, 2131−2137.
(3) (a) Nguyen, J. Q.; Iverson, B. L. *J. Am. Chem. Soc.* **1999**, *121*, 2639−2640. (b) Zhang, W.; Horoszewski, D.; Decatur, J.; Nuckolls, C. *J. Am. Chem. Soc.* **2003**, *125*, 4870−4873. (c) Wang, W.; Li, L.-S.; Helms, G.; Zhou, H.-H.; Li, A. D. Q. *J. Am. Chem. Soc.* **2003**, *125*, 1120−1121. (d) Wang, W.; Wan, W.; Zhou, H.-H.; Niu, S.; Li, A. D. Q. *J. Am. Chem. Soc.* **2003**, *125*, 5248−5249. (e) Ghosh, S.; Ramakrishnan, S. *Angew. Chem., Int. Ed.* **2004**, *43*, 3264−3268.
(4) (a) Brunsveld, L.; Folmer, B. J. B.; Sijbesma, R. P.; Meijer, E. W. *Chem. Rev.* **2001**, *101*, 4071−4098. (b) ten Cate, A. T.; Sijbesma, R. P. *Macromol. Rapid Commun.* **2002**, *23*, 1094−1112. (c) Ciferri, A. *Macromol. Rapid Commun.* **2002**, *23*, 511−529. (d) Lehn, J.-M. *Polym. Int.* **2002**, *51*, 825−839.
(5) (a) Hirschberg, J. H. K.; Brunsveld, L.; Ramzi, A.; Vekemans, J. A. J. M.; Sijbesma, R. P.; Meijer, E. W. *Nature* **2000**, *407*, 167−170. (b) Brunsveld, L.; Vekemans, J. A. J. M.; Hirschberg, J. H. K.; Sijbesma, R. P.; Meijer, E. W. *Proc. Natl. Acad. Sci. U.S.A.* **2002**, *99*, 4977−4982. (c) Hirschberg, J. H. K.; Koevoets, R. A.; Sijbesma, R. P.; Meijer, E. W. *Chem.*—Eur. J. **2003**, *9*, 4222−4231.

10.1021/cm0510413 CCC: $30.25
Published on Web 07/23/2005

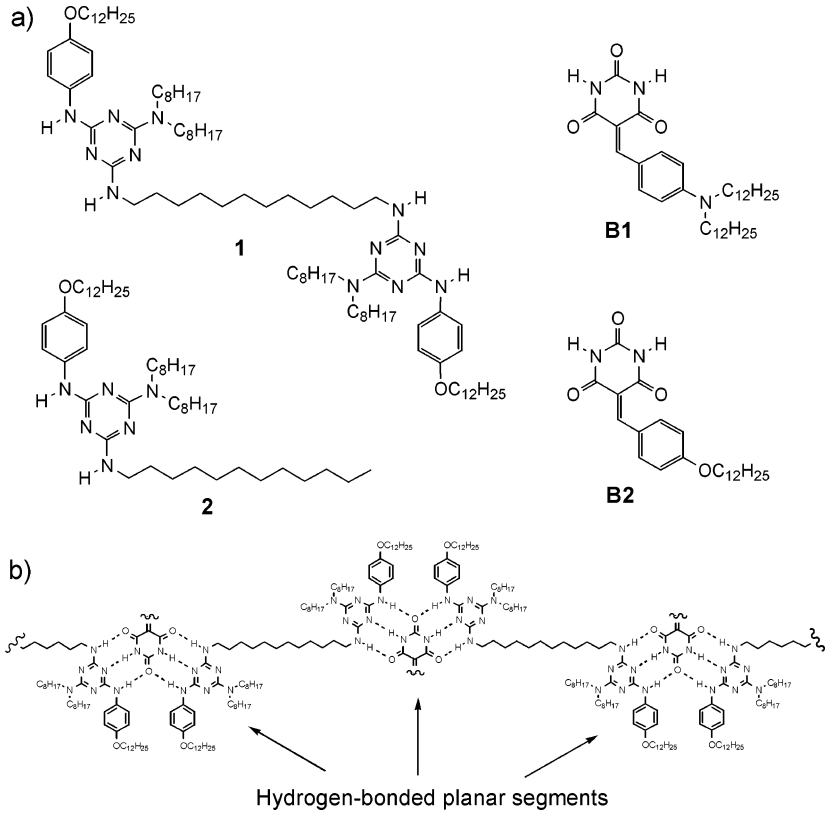

Figure 1. (a) Structures of bis(melamine) **1**, reference monotopic melamine **2**, and barbiturate-type merocyanines **B1** and **B2**. (b) Possible structure of the supramolecular polymer.

to obtain ordered macroscopic structures. We herein report that the well-defined macroscopic structure of our supramolecular polymers can be indeed induced by the use of barbiturate-type dipolar merocyanine dyes **B1** and **B2** as partners of **1**.[9] Moreover, the resulting different macroscopic structure resulted in dramatically different rheological behavior of the supramolecular polymers in aliphatic solvents (gellike materials).

Experimental Section

Materials. The synthesis of all compounds was previously reported.[7] Supramolecular polymer solutions were prepared as follows: an equimolar blend of bis(melamine) **1** and merocyanine **B1** or **B2** was dissolved in an appropriate amount of aliphatic solvent by refluxing in capped glass vial. When the vial was cooled to room temperature, the solution immediately turned viscous fluid or gel at high concentrations. Samples for UV−vis and DLS measurements were prepared by diluting the above gellike materials.

Methods. Rheological measurements were conducted on an Anton Paar modular compact rheometer (Physica) equipped with a parallel plate geometry.

T_2 measurements of the supramolecular solutions were conducted on JEOL MU25 pulse NMR spectrometer using glass tubes of diameter 10 mm. The Carr Purcel Meiboom Gill pulse sequence was employed to obtain the T_2 of the samples.

DLS measurements were performed on a Zetasizer Nano (Malvern Instruments Ltd.) equipped with a He−Ne laser (633 nm, 4.0 mW). Supramolecular polymer solutions were heated and then filtered using a Millipore membrane filter (200 nm pore size) before measurements.

(6) (a) Hoeben, F. J. M.; Jonkheijm, P.; Meijer, E. W.; Schenning, A. P. H. J. *Chem. Rev.* **2005**, *105*, 1491−1546. (b) Schoonbeek, F. S.; van Esch, J. H.; Wegewijs, B.; Rep, D. B. A.; de Haas, M. P.; Klapwijk, T. M.; Kellogg, R. M.; Feringa, B. L. *Angew. Chem., Int. Ed.* **1999**, *38*, 1393−1397. (c) Würthner, F.; Thalacker, C.; Sautter, A.; Schärtl, W.; Ibach, W.; Hollricher, O. *Chem.*—Eur. J. **2000**, *6*, 3871−3886. (d) El-ghayoury, A.; Schenning, A. P. H. J.; van Hal, P. A.; van Duren, J. K. J.; Janssen, R. A. J.; Meijer, E. W. *Angew. Chem., Int. Ed.* **2001**, *40*, 3660−3663. (e) Schenning, A. P. H. J.; Jonkheijm, P.; Peeters, E.; Meijer, E. W. *J. Am. Chem. Soc.* **2001**, *123*, 409−416. (f) Ajayaghosh, A.; George, S. J.; Praveen, V. K. *Angew. Chem., Int. Ed.* **2003**, *42*, 332−335. (g) Würthner, F.; Yao, S.; Beginn, U. *Angew. Chem., Int. Ed.* **2003**, *42*, 3247−3250. (h) Hoeben, F. J. M.; Herz, L. M.; Daniel, C.; Jonkheijm, P.; Schenning, A. P. H. J.; Silva, C.; Meskers, S. C. J.; Beljonne, D.; Phillips, R. T.; Friend, R. H.; Meijer, E. W. *Angew. Chem., Int. Ed.* **2004**, *43*, 1976−1979. (i) Sugiyasu, K.; Fujita, N.; Shinkai, S. *Angew. Chem., Int. Ed.* **2004**, *43*, 1229−1233. (j) George, S. J.; Ajayaghosh, A.; Jonkheijm, P.; Schenning, A. P. H. J.; Meijer, E. W. *Angew. Chem., Int. Ed.* **2004**, *43*, 3422−3425. (k) Würthner, F.; Chen, Z.; Hoeben, F. J. M.; Osswald, P.; You, C.-C.; Jonkheijm, P. Herrikhuyzen, J. v.; Schenning, A. P. H. J.; van der Schoot, P. P. A. M.; Meijer, E. W.; Beckers, E. H. A.; Meskers, S. C. J.; Janssen, R. A. J. *J. Am. Chem. Soc.* **2004**, *126*, 10611−10618. (l) Messmore, B. W.; Hulvat, J. F.; Sone, E. D.; Stupp, S. I. *J. Am. Chem. Soc.* **2004**, *126*, 14452−14458. (m) Thalacker, C.; Miura, A.; De Feyter, S.; De Schryver, F. C.; Würthner, F. *Org. Biomol. Chem.* **2005**, *3*, 414−422. (n) Ajayaghosh, A.; George, S. J. *J. Am. Chem. Soc.* **2001**, *123*, 5148−5149. (o) Ajayaghosh, A.; George, S. J. *Chem.*—Eur. J. **2005**, *11*, 3217−3227.

(7) Yagai, S.; Higashi, M.; Karatsu, T.; Kitamura, A. *Chem. Mater.* **2004**, *16*, 3582−3585.

(8) (a) Inoue, K.; Ono, Y.; Kanekiyo, Y.; Ishi-I, T.; Yoshihisa, K.; Shinkai, S. *J. Org. Chem.* **1999**, *64*, 2933−2937. (b) Berl, V.; Krische, M. J.; Huc, I.; Lehn, J.-M.; Schmutz, M. *Chem.*—Eur. J. **2000**, *6*, 1938−1946. (c) Ikeda, M.; Nobori, T.; Schmutz, M.; Lehn, J-.M. *Chem.*—Eur. *J.* **2005**, *11*, 662−668.

(9) (a) Yang, W.; Jiang, Y.; Chai, X.; Li, T.; Fu, L.; Zhang, H. *Sci. China* **2000**, *43*, 555−560. (b) Ahuja, R.; Caruso, P.-L.; Möbius, D.; Paulus, W.; Ringsdorf, H.; Wildburg, G. *Angew. Chem., Int. Ed. Engl.* **1993**, *32*, 1033−1036. (c) Bohanon, T. M.; Caruso, P.-L.; Denzinger, S.; Fink, R.; Möbius, D.; Paulus, W.; Preece, J. A.; Ringsdorf, H.; Schollmeyer, D. *Langmuir* **1999**, *15*, 174−184. (d) Huang, X.; Li, C.; Jiang, S.; Wang, X.; Zhang, B.; Liu, M. *J. Am. Chem. Soc.* **2004**, *126*, 1332−1323. (e) Würthner, F.; Yao, S.; Heise, B.; Tschierske, C. *Chem. Commun.* **2001**, 2260−2261.

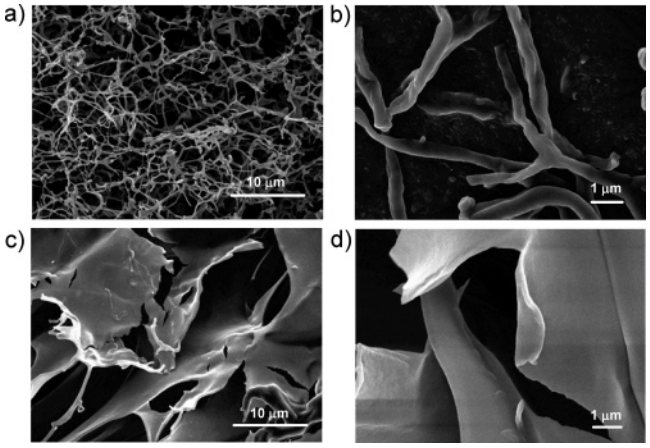

Figure 2. FE-SEM images of supramolecular polymers **1·B1** (a, b) and **1·B2** (c, d), freeze-dried from their cyclohexane solutions (c = 2 mM).

Electron microscopic observation was conducted using a JEOL JSM-6330F field emission scanning electron microscopy. The sample solution was placed on carbon grid and then frozen by liquid N_2. The vacuum-dried samples were coated by osmium before observations.

Results and Discussion

Macroscopic Structure of the Supramolecular Polymers. Merocyanine dyes **B1** and **B2** are capable of self-aggregating via hydrogen-bonding as well as dipolar interactions, and thereby, they are sparingly soluble in the least polar solvents such as cyclohexane and methylcyclohexane (MCH) even at refluxing temperature, while they become highly soluble (~100 mM) when the solution was refluxed in the presence of 1 equiv of **1**. This indicates the formation of 1:1 hydrogen-bonded complexes between **1** and the dyes. As the result of the propagated supramolecular polymer networks, concentrated cyclohexane solution of **1·B1** and **1·B2** immediately turned into transparent organogels at ambient temperature. Interestingly, the minimum gelation concentration (MGC) is drastically different in the two supramolecular polymers: 16 mM (31.3 g/L) for **1·B1** and 1 mM (1.78 g/L) for **1·B2**. This large difference in MGC might be due to the difference in the macroscopic structure of the self-organized supramolecular polymers. Therefore, the macroscopic structures of **1·B1** and **1·B2** in cyclohexane (c = 2 mM) were freeze-dried and observed by field emission scanning electron microscopy (FE-SEM).

In Figure 2 are compared the FE-SEM images of the supramolecular polymers. Surprisingly, despite their conformational flexibility in the long alkyl linkage in **1**, both the supramolecular polymers showed well-defined macroscopic structures. **1·B1** exhibited an entangled fibrous network with the diameters less than 1 μm (Figure 2a,b), typical of low-molecular weight organogels. In clear contrast, **1·B2** showed a two-dimensional sheetlike structure with the thickness of approximately 100 nm (Figure 2c,d). Analogous sheetlike structures have been reported in several "weak" organogel systems.[10] These macroscopic morphologies of the supramolecular polymers are basically not affected by the concentration of the solutions, indicating the intrinsic propensity of the supramolecular polymers to hierarchically organize into specific macroscopic structures.

Interestingly, the cyclohexane solution of **1·B2** showed birefringence (formation of the lyotropic mesophase) whereas **1·B1** did not. In Figure 3 are shown the optical microscopic images of 10 mM solutions under polarized light. Clear birefringence in the **1·B2** solution (Figure 3a) indicates anisotropic orientation of the flexible supramolecular polymers in the sheets. On the other hand, a solution of **1·B1** exhibited no birefringence until the solvent was completely evaporated (Figure 3b). This implied that the hierarchical organization of **1·B1** is less directional due to the lack of specific interchain interactions.

Combined with the MGC values, the above macroscopic structures reveal that the sheetlike structure of **1·B2** is more effective to suppress the solvent flow than the fibrous structure of **1·B1**. However, the spin−spin relaxation time (T_2) of cyclohexane protons in the supramolecular polymer solutions (c = 6 mM, 25 °C) is 1.41 s for **1·B1** and 2.70 s for **1·B2**, indicating that the diffusion of the solvent molecule is much suppressed by the former (fibrous structure). This result manifests that the macroscopic sheets composed of **1·B1** suppress solvent flow by simply compartmentalizing the solvent molecules. On the contrary, the fine fibrous network of **1·B2** has a much larger contact area, more firmly trapping the solvent molecules via the specific solvent−solute interactions (e.g., surface tension).[11]

Rheological Behavior of the Supramolecular Polymer Solutions. Together with the drastic difference in the macroscopic structures described in the previous section, the mechanical properties of the two supramolecular polymer solutions are dramatically different. Preliminary observation suggested that the cyclohexane gel of **1·B1** is insensitive to mechanical agitation whereas that of **1·B2** is very fragile against mechanical agitation.[7] From the view of material sciences, it is quite appealing that the simple alteration of the dye molecules blended with **1** affects the rheological properties of the resulting soft materials.

To assess the dye-dependent mechanical properties of the supramolecular polymer solutions in detail, dynamic rheological measurements were conducted for the supramolecular polymers in cyclohexane (c = 6 mM) using a stress-controlled rheometer (Figure 4). Both the supramolecular polymer solutions behave as non-Newtonian fluids as shown by linear decrease of complex viscosity (η^*) with increase of the strain frequency. Additionally, the storage (G') and the loss (G'') moduli slightly depend on the frequency, showing the viscoelastic behavior of the supramolecular polymer solutions. The complex viscosity of the **1·B1** solution is roughly 1 order of magnitude smaller than that of the **1·B2** solution, consistent with the drastic difference in their MGC values.

Figure 5 shows the dependencies of the moduli on oscillatory strain amplitude (frequency = 1 rad·s^{-1}). G' (red open circles) and η^* (red closed circles) of the **1·B1** solution showed wide plateau region until the strain amplitude reached

(10) The same sheetlike structure has been observed in weaker organogel systems: (a) Jung, J. H.; Ono, Y.; Shinkai, S. *Langmuir* **2000**, *16*, 1643−1649. (b) Watanabe, Y.; Miyasou, T.; Hayashi, M. *Org. Lett.* **2004**, *6*, 1547−1550.

(11) Wang, R.; Geiger, C.; Chen, L.; Swanson, B.; Whitten, D. G. *J. Am. Chem. Soc.* **2000**, *122*, 2399−2400.

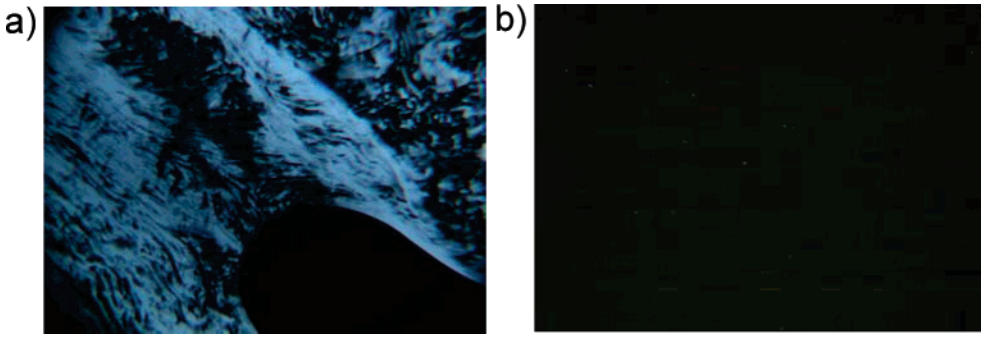

Figure 3. Optical micrographs of supramolecular polymers **1·B2** (a) and **1·B1** (b) in cyclohexane (c = 10 mM) with crossed polarizers.

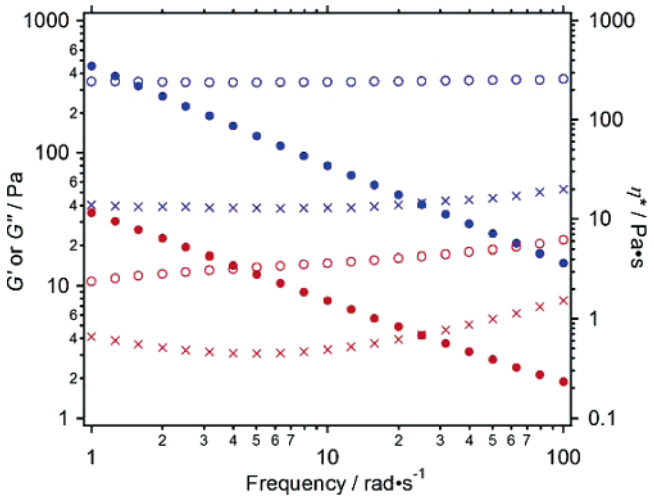

Figure 4. Storage modulus (G', ○), loss modulus (G'', ×), and complex viscosity (η^*, ●) versus angular frequency for supramolecular polymers **1·B1** (red marks) and **1·B2** (blue marks) in cyclohexane (c = 6 mM) at 15 °C. Strain amplitude = 0.5%.

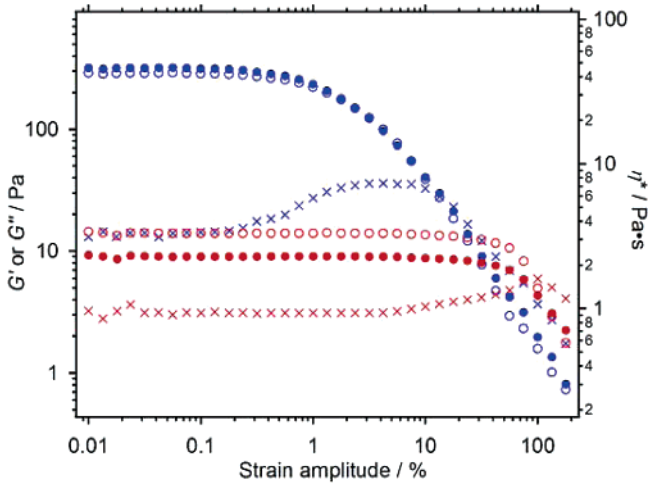

Figure 5. Storage modulus (G', ○), loss modulus (G'', ×), and complex viscosity (η^*, ●) at 1 rad•s^{-1} versus shear strain amplitude for supramolecular polymers **1·B1** (red marks) and **1·B2** (blue marks) in cyclohexane (c = 6 mM) at 15 °C.

ca. 30%, indicating the presence of polymer-like elastic nature derived from the entangled fibrous network. On the other hand, G' (blue open circles) and η^* (blue closed circles) of the **1·B2** solution were independent of the strain amplitude only in low strain regime and started to drop already at the strain amplitude around 1%. The very fragile nature can be attributed to the mechanical collapse of the macroscopic sheets observed by FE-SEM, which in turn leads to the

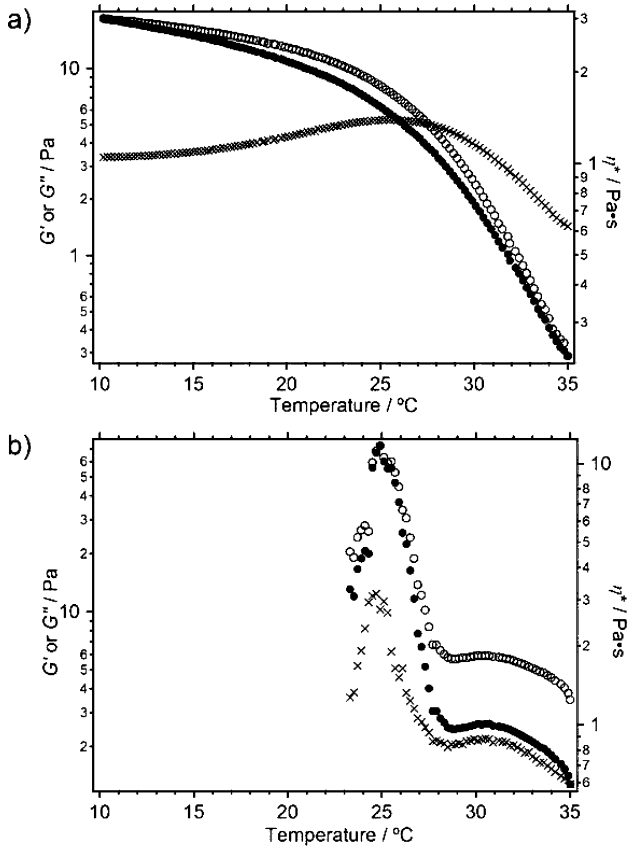

Figure 6. Storage modulus (G', ○), loss modulus (G'', ×), and complex viscosity (η^*, ●) versus temperature for supramolecular polymers **1·B1** (a) and **1·B2** (b) in cyclohexane (c = 6 mM). Frequency = 1 rad•s^{-1}. Shear strain amplitude = 1%.

leakage of the compartmentalized solvents. It should be noted that at high strain regime (>20%), G' and η^* of the **1·B1** solution prevail that of the **1·B2** solution. Thus, these dramatically different mechanical properties of the supramolecular polymer solutions can be well-related to their macroscopic structures observed by FE-SEM.

Finally, the growth of the macroscopic fibers (**1·B1**) and sheets (**1·B2**) was investigated by means of temperature-sweep (35 → 10 °C) rheological measurements (Figure 6). At 35 °C, the complex viscosities of both the supramolecular polymer solutions are far below 1 Pa•s, indicating the absence of macroscopic structures to confine the solvent molecules. Upon cooling, the **1·B1** solution showed gradual increase of G' and η^* (Figure 6a), indicating the ambient formation of the macroscopic fibers via weak cohesive force between the individual supramolecular polymers. In sharp contrast,

when **1·B2** solution was cooled from 35 °C, G' and η^* gradually increase and reached a narrow plateau from 30 to 28.5 °C (Figure 6b). Remarkably, after the plateau, the moduli abruptly rose, indicating that the formation of the sheet is highly precipitous process. Further cooling resulted in reproducible sharp drop of the moduli at 25 °C probably due to the shrinking accompanying macroscopic gelation, hampering measurements at lower temperature. This characteristics behavior in the formation of the sheets may originate from the cooperative association of the supramolecular polymer **1·B2**.

Supramolecular Polymers in Dilute Solutions. As described above, the macroscopic structures and the resulting rheological properties of **1·B1** and **1·B2** are dramatically different despite their close structural relation. Moreover, the results of temperature-sweep rheological measurements as shown in Figure 6 clearly demonstrated that the hierarchical organization of the two supramolecular polymers is driven by the different noncovalent forces. Here, it is worthy to invoke the very different electronic characters of **B1** and **B2** due to the strength of the electron-donating ability of the aromatic substituents: the didodecylamino group of **B1** is a stronger electron-donating substituent than the dodecyloxy group of **B2**. Li et al. suggest that such electronic difference leads to the different stacking arrangements of these dyes, i.e., face-to-face (*H*-aggregate) stacking in **B1** and offset stacking (*J*-aggregate) in **B2**.[9a] If such intrinsic stacking propensities of the dyes are operative when they are embedded in the hydrogen-bonded planar segments, the two supramolecular polymers may adopt different secondary structures and thereby self-organized into dramatically different macroscopic structures.

To investigate the above possibility, supramolecular polymerizations were investigated by UV−vis spectroscopy under diluted conditions (micromolar regime). Initially, to confirm the presence of nanometer-size supramolecular polymers in a diluted condition, dynamic light scattering (DLS) measurements were conducted for 250 μM cyclohexane solutions of **1·B1** and **1·B2**. The average sizes of the aggregates at 20 °C reached 90 nm for **1·B1** and 400 nm for **1·B2**, respectively, demonstrating the formation of extended supramolecular polymers even at the diluted condition. Remarkably, the average aggregate size of **1·B2** is 4-fold larger than that of **1·B1** even under the same measurement conditions. Since the hydrogen-bonding strength of barbiturate-type merocyanines is not amenable to their molecular structures,[12] the significant difference in the aggregate sizes must arise from the difference in the secondary structure of the supramolecular polymers and not be derived from the difference in degree of polymerization.

By virtue of its rich push−pull character, **B1** shows moderate UV−vis spectral change upon hydrogen bonding with **1**.[13] At low concentration range around 5 μM, the intramolecular charge transfer (ICT) absorption band of **B1** was observed at λ_{max} = 467 nm (red curve in Figure 7a), which is less structured and red-shifted from that of **B1** alone

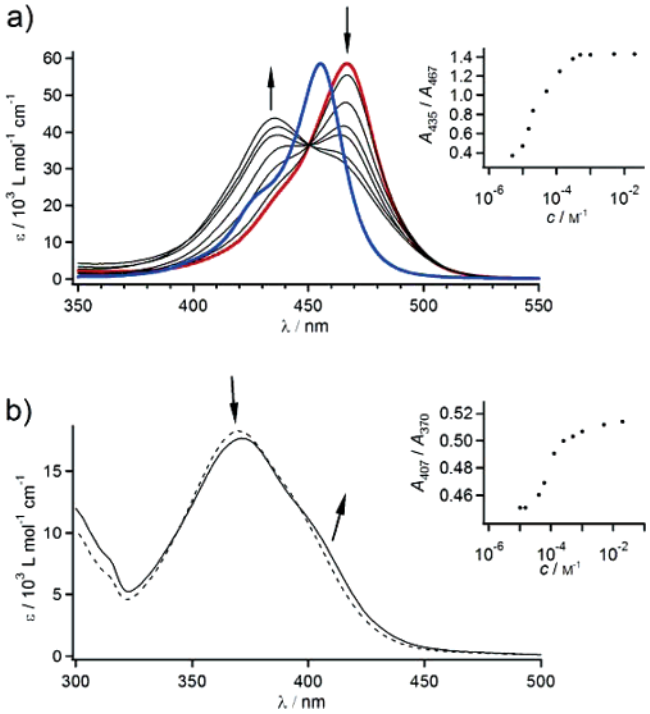

Figure 7. (a) Concentration-dependent (from 5 to 500 μM) UV−vis spectra of a 1:1 molar mixture of **1** and **B1** in cyclohexane. The spectra of a 5 μM mixture and **B1** alone are shown by red and blue curves, respectively. Inset: plot of the ratio of the absorption intensities at 435 and 467 nm (A_{407}/A_{370}) versus the concentration. (b) UV−vis spectra of a 1:1 molar mixture of **1** and **B2** in cyclohexane at concentrations of 50 μM (dashed curve) and 2.0 mM (solid curve). Inset: plot of the ratio of the absorption intensities at 407 and 370 nm (A_{407}/A_{370}) versus the concentration (from 10 mM to 20 mM). Arrows indicate the changes upon increasing concentrations.

in cyclohexane (λ_{max} = 456 nm, blue curve). These small changes can be attributed to the complementary hydrogen-bonding interaction with **1**. Interestingly, dilution of the **1·B1** solution revealed that **B1** entirely complexes with **1** even at very low concentrations around 3 μM. This is in contrast to the 2 + 1 complex of monotopic melamine **2** with **B1** (**2·B1·2**), where only 20% of **B1** complexes with **2** at 10 μM from UV−vis analysis. These observations strongly suggests that the formation of highly stable closed species such as Hamilton-type complex between **1** and **B1** at the diluted conditions.[7] Interestingly, upon increasing concentration, a new blue-shifted band (*H*-band) with λ_{max} = 435 nm grew in compensation for the decrease of the 467-nm band (arrows in Figure 7a), indicating the formation of *H*-aggregates.[9b−e,14] The growth of the *H*-band starts at ca. 20 μM and saturated already at a concentration of ca. 500 μM, over which the absorption spectra almost follow Beer's law (inset in Figure 7a). Such a spectral transition in the narrow concentration range clearly excludes the simple growth of small cyclic species into extended structures. Instead, it can be proposed that concentration-induced ring-opening of small closed species occurred and the resulting extended supramolecular polymer folded into the secondary structure as a result of intrachain *H*-aggregation of **B1** embedded in the hydrogen-bonded segments (Scheme 1a).

In sharp contrast, the UV−vis spectral change of **B2** upon hydrogen bonding with **1** is considerably small due to its

(12) Würthner, F.; Yao, S. *J. Org. Chem.* **2003**, *68*, 8943−8949.
(13) Prins, L. J.; Thalacker, C.; Würthner, F.; Timmerman, P.; Reinhoudt, D. N. *Proc. Natl. Acad. Sci. U.S.A.* **2002**, *99*, 4814−4817.
(14) Würthner, F.; Yao, S.; Debaerdemaeker, T.; Wortmann, R. *J. Am. Chem. Soc.* **2002**, *124*, 9431−9447.

Scheme 1. Proposed Mechanism for the Formation of Secondary Structures from Supramolecular Polymers 1·B1 via Intrachain Association (a) and 1·B2 via Interchain Association (b)[a]

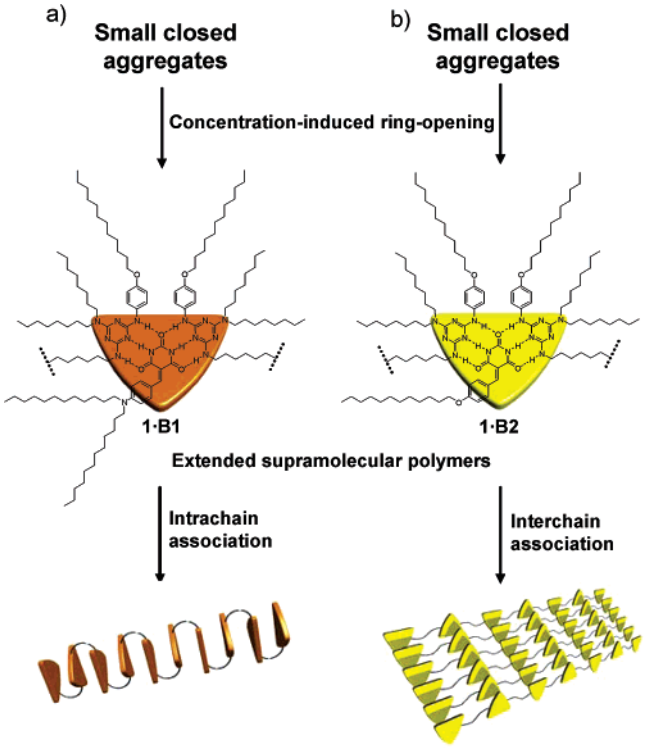

[a] The yellow and orange triangles show the hydrogen-bonded planar segments.

poor push−pull character. At the concentrations below 50 μM ([**1**] = [**B1**]), the ICT absorption band of **B2** was always observed at λ_{max} = 370 nm and the spectrum is almost independent of the concentration (Figure 7b). This indicates that the absorption property of **B2** is unaffected by hydrogen bonding with **1**. However, closer inspection revealed that upon increasing the concentration to 2 mM, the shoulder at the red side of the ICT band became more pronounced (arrows in Figure 7b). Though the absorption spectral change is considerably small, the plot of the ratio of the absorption intensity at 407 and 370 nm versus the concentrations revealed that the spectral change occurs in the wide concentration range (inset in Figure 7b). This result implies that the extension of supramolecular polymer is accompanied by the interchain association of embedded **B2**, resulting in the two-dimensional propagation of the supramolecular polymers (Scheme 1b). Combined with the intrinsic propensity of **B2** to form *J*-aggregate, the red-shifted absorption band strongly suggests that the stacking arrangement in the present case is also *J*-type. The larger aggregate size of **1·B2** (400 nm) than **1·B1** (90 nm) observed in the DLS study is fully in agreement with the extended secondary structure of **1·B2** by the interchain association in comparison with the pleated secondary structure of **1·B1**. The origin of interchain association in **1·B2** instead of the intrachain association like in **1·B2** is believed to be the conformational disadvantage upon the formation of folded secondary structure by the offset-stacking of hydrogen-bonded planar segments.

Given the above UV−vis results, dramatic difference in the macroscopic structure and rheological behavior of the supramolecular polymers **1·B1** and **1·B2** can be attributed to the difference in their nanometer scale secondary structures. Folding of supramolecular polymer **1·B1** affords a rodlike secondary structure surrounded by the aliphatic chains (Scheme 1a). Such a rodlike structure further assembles into fibrous macroscopic structures via weak, less directional van der Waals interaction between the exterior aliphatic chains. This is consistent with the ambient propagation of the fibers of **1·B1** in the temperature-sweep rheological experiment (Figure 6a) as well as the absence of birefringence under the polarized light (Figure 3b). In contrast, interchain association of **1·B2** (Scheme 1b) is fully consistent with the precipitous formation of sheetlike structure in the temperature-sweep rheological measurements (Figure 6b) as well as the anisotropic orientation of the supramolecular polymers demonstrated by the clear birefringent texture under polarized light (Figure 3a). It is quite interesting to note that the nanometer scale secondary structures of the two supramolecular polymers, i.e., one-dimensional rodlike structure and two-dimensional sheetlike structure, can be amplified to the macroscopic structures observed by FE-SEM.[15]

Conclusion

In summary, this study demonstrated a unique strategy to obtain well-defined macroscopic structures from random coil supramolecular polymers using dipolar hydrogen-bonding dyes. The two different macroscopic structures, viz., fiber and sheet, were obtained by the incorporation of two different dyes which structurally resemble each other but differ in their electronic characters. As a consequence of the dramatically different macroscopic structures, the corresponding gellike soft materials in aliphatic solvent showed dramatically different rheological behaviors. From the UV−vis studies, it is strongly suggested that *H*-aggregation (face-to-face stacking) and *J*-aggregation (offset stacking) of the dye molecules embedded in the hydrogen-bonded planar segments control the secondary interaction of the supramolecular polymers, i.e., intrachain association (folding) and interchain association, respectively.[16] Such supramolecular polymers featuring dramatically different secondary structure are believed to hierarchically organize into the fibrous and sheetlike macroscopic structures. Thus, a diverse kind of dye-incorporated self-organized fibers and sheets can be obtained by mixing our bis(melamine) with various diimide-functionalized dyes.[6c,m,12] Such soluble supramolecular polymeric materials featuring organized dye assemblies have a potential for expansion to processible optoelectronic soft materials.

(15) Shinkai et al. reported that *J*- and *H*-aggregates of the hydrogen-bonding porphyrin derivatives exhibit sheet and fiber superstructures, respectively: Shirakawa, M.; Kawano, S.; Fujita, N.; Sada, K.; Shinkai, S. *J. Org. Chem.* **2003**, *68*, 5037−5044.

(16) Other supramolecular polymers of which secondary structures can be tunable by the second component: (a) Yamaguchi, T.; Ishii, N.; Tashiro, K.; Aida, T. *J. Am. Chem. Soc.* **2003**, *125*, 13934−13935. (b) Kim, H.-J.; Zin, W.-C.; Lee, M. *J. Am. Chem. Soc.* **2004**, *126*, 7009−7014. (c) Shirakawa, M.; Fujita, N.; Shinkai, S. *J. Am. Chem. Soc.* **2004**, *126*, 9902−9903. (d) Hardy, J. G.; Hirst, A. R.; Smith, D. K.; Brennan, C.; Ashworth, I. *Chem. Commun.* **2005**, 385−387. (e) Hirst, A. R.; Smith, D. K.; Feiters, M. C.; Geurts, H. P. M.; Wright, A. C. *J. Am. Chem. Soc.* **2003**, *125*, 9010−9011.

At the same time, the relationship between the intrinsic self-aggregation property of the incorporated dyes and the secondary structure of the supramolecular polymers as well as the resulting macroscopic structures is an intriguing issue for advancing research.

Acknowledgment. The authors are grateful to Nihon SiberHegner K.K. Co. Ltd. and Dr. Chiaki Ishii (Chiba University)for the rheological measurements, Prof. Dr. Hitoshi Tamiaki and Dr. Yoshitaka Saga (Ritsumeikan University) for the DLS measurements, and Hiroko Seki (Chemical Analysis Center of Chiba University) for the T_2 measurements. The financial support from Tokuyama Science Foundation and The Asahi Glass Foundation is gratefully acknowledged.

CM0510413